Stratifications of the Euclidean motion group with applications to robotics

Maria Alberich-Carramiñana[(a,b)], Víctor González[(a)], Federico Thomas[(b)], and Carme Torras[(b)]

(a) Department of Applied Mathematics I
Universitat Politècnica de Catalunya (UPC)
Avda. Diagonal 647, 08028-Barcelona, Spain.

(b) Institut de Robòtica i Informàtica Industrial (CSIC-UPC)
Llorens i Artigas 4-6, 08028-Barcelona, Spain.

Corresponding author:
Maria Alberich-Carramiñana
E-mail: maria.alberich@upc.edu
Tel. 34-93-4016550
Fax. 34-93-4011713

Stratifications of the Euclidean motion group with applications to robotics

Abstract

In this paper we derive stratifications of the Euclidean motion group, which provide a complete description of the singular locus in the configuration space of a family of parallel manipulators, and we study the adjacency between the strata. We prove that classically known cell decompositions of the flag manifold restricted to the open subset parameterizing the affine real flags are still stratifications, and we introduce a refinement of the classical Ehresmann-Bruhat order that characterizes the adjacency between all the different strata. Then we show how, via a four-fold covering morphism, the stratifications of the Euclidean motion group are induced.

Keywords: Flag manifold, stratification, Euclidean motion group, cell decomposition, singular locus, parallel manipulators.

1 Introduction

The spatial fully-parallel manipulator [6] can abstractly be described as two bodies, *base* and *platform*, joined by six segments (or *legs*) of variable lengths. The points where the legs are located on the base and the platform are called *endpoints*. The configuration space which describes all possible platform locations with respect to the base is $\mathbb{R}^3 \times SO_3(\mathbb{R})$, the *Euclidean motion group*. It is a differentiable manifold of dimension 6, and this is why the platform and the base are joined by six legs: to achieve the six degrees of freedom which enable the platform to reach every point in the configuration space.

The direct (or forward) kinematics problem consists in finding the location of the platform with respect to the base from the lengths of the six legs, that is, in determining the pre-images of the (differentiable) map

$$\Phi : \mathbb{R}^3 \times SO_3(\mathbb{R}) \longrightarrow \mathbb{R}^6 \,. \tag{1}$$

The set of configurations at which Φ is singular is called the *singular locus* of the manipulator. For a detailed formulation of kinematics mappings and their singularities, the reader is referred to [7].

Technically, singular configurations cause problems: at such configurations the derivative of Φ does not have full rank, and hence the manipulator loses some degree(s) of constraint (or gains some degree(s) of freedom) and becomes uncontrollable. Furthermore, the actuator forces in the legs may become very large, which could result in a breakdown of the robot. Therefore it is desirable to have a complete overview of the singular locus of the manipulator. Such a complete characterization of the singular locus in the configuration space would permit identifying the non-singular regions separated by singularities, the restriction on manoeuverability occurring in each singular region, as well as the adjacency between all non-singular and singular regions [6]. This would be most useful for manipulator design, including the use of redundant actuators to eliminate certain singularities, and also to plan trajectories away from singularities, or crossing them in a controlled way.

In this paper we derive stratifications of the Euclidean motion group, from classically known stratifications of the flag manifold, which provide a complete description of the singular locus in the configuration space of a family of parallel manipulators, called *flagged manipulators*. This class of robots was first identified in [20], and is worked out in detail in [2] (being expanded from a basic manipulator) where it is shown to contain large subfamilies of parallel and three-legged spatial manipulators (by substituting 2-leg groups by different serial chains).

The stratifications of $\mathbb{R}^3 \times SO_3(\mathbb{R})$ derived in the present paper have become a valuable tool in the field of robot kinematics and have been the source of inspiration of several works in that field: they were already applied in [20] to give explicitly all the singular strata and their connectivity, for all members in the class of flagged manipulators, irrespective of the metrics of each particular robot design. Moreover, [20] also showed that these strata admit an easy control strategy to cross them, because it is possible

to assign local coordinates to each stratum (in the configuration space of the manipulator) which correspond to uncoupled rotations and/or translations. The applicability of these stratifications to come up with robot designs which admit control strategies free of singularities has been exploited as well: in [1] redundant actuators have been introduced by adding an extra leg to a given flagged manipulator, which admits a control strategy (by appropriately choosing which leg remains passive) that completely avoids singularities.

The organization of the paper is as follows. Section 2, after recalling some concepts and results concerning the manifold parameterizing the projective real flags, is devoted to derive stratifications of the space parameterizing the affine real flags, and to determine the adjacency between those strata. Section 3 shows how the stratifications for the affine real flags induce stratifications of the Euclidean motion group, and studies the adjacency between the higher dimensional strata. Then, in Section 4, we explain the connection of the stratifications of the Euclidean motion group derived in this paper with the kinematics of flagged robot manipulators. Finally, Section 5 sketches other possible applications of the developed stratifications.

2 From projective real flags to affine real flags

It is classically known that the flag manifold, which parameterizes the set of projective flags, admits well-behaved topological decompositions, namely stratifications (in fact, cell decompositions); see [16], [10]. Moreover, the classical Ehresmann-Bruhat order describes all the possible degenerations of a pair of flags in a linear space V under linear transformations of V. We shall deal with the flag manifold over $\mathbb{R}^n$, that is, the linear space $V = \mathbb{R}^n$, motivated, as explained in the introduction, by the issues in the field of robot kinematics. This same motivation leads us to consider affine flags. In this section we prove that some stratifications of the flag manifold restricted to the set of the affine flags are still stratifications, and we introduce a refinement of the classical Ehresmann-Bruhat order that characterizes the adjacency between all the different strata, that is, describes all the possible degenerations of any configuration to more special ones.

Given a positive integer n, the *flag manifold* $\mathcal{F}lag(n+1)$ over $\mathbb{R}^{n+1}$ parameterizes the set of flags in $\mathbb{P}^n = \mathbb{P}^n(\mathbb{R})$, where a *flag* in $\mathbb{P}^n$ is a sequence $(V_0, \ldots, V_n)$ of projective subspaces with $V_0 \subset \cdots \subset V_n = \mathbb{P}^n$ and $\dim V_i = i$ for $1 \leq i \leq n$. The nested subspaces between the point V_0 and the hyperplane

V_{n-1} defining a flag will be referred to as *flag features*. Once a distinguished hyperplane H_∞ in $\mathbb{P}^n$ is chosen, the *affine flags* are the flags $(V_0, \ldots, V_n)$ in $\mathbb{P}^n$ satisfying $V_0 \notin H_\infty$. Let $\mathcal{F}_{\mathcal{A}}(\mathbb{P}^n)$ denote the open subset of the affine flags in $\mathcal{F}lag(n+1)$.

The notion of well-behaved topological decomposition is formalized in the following definition. A *stratification* of a subset S of a smooth manifold M is a partition $S = \cup_{i \in I} S_i$ such that: I is finite, S_i is a smooth submanifold of M for any $i \in I$, and if $S_i \cap \overline{S}_j \neq \emptyset$, then $S_i \subset \overline{S}_j$, where $\overline{S}_j$ stands for the closure of S_j. The S_i's are called *strata*. The third boundary condition guarantees that the boundary of a stratum is the union of the entire strata which are not disjoint from it, that is, there are not "exceptional" degenerations between strata: if a configuration of a stratum S_i is a degeneration of a configuration of a stratum S_j, then any configuration in S_i can be considered as a degeneration of some configuration of S_j.

Next, let us summarize the classical theory on stratifications of the flag manifold, following [9] as main reference. Fix a *reference flag* $(V_0, \ldots, V_n)$. Let Σ_{n+1} be set of permutations of $n+1$ elements, and consider $w \in \Sigma_{n+1}$.

Definition 1 (Bruhat or Schubert cell). *The Bruhat or Schubert cell B^w associated with the permutation w is the set of all flags whose flag features have incidence relations with the reference flag determined by w in the following way:*

$$B^w = \{(V_0^*, \ldots, V_n^*) \in \mathcal{F}\text{lag}(n+1) : \dim(V_p^* \cap V_q) = r_w(p,q) \text{ for } 1 \leq p, q \leq n\}$$

where $r_w(p,q) = \#\{i \leq p : w(i) \leq q\} - 1$.

Given a flag $(V_0, \ldots, V_n)$, we can choose a projective reference frame $\{\mathbf{a}_1, \ldots, \mathbf{a}_{n+1}; \mathbf{a}\}$ of $\mathbb{P}^n$ satisfying $\mathbf{a}_i \in V_{i-1}$ for $1 \leq i \leq n+1$, which will be called *a frame attached to the flag* $\mathcal{V}$. To each permutation w in Σ_{n+1}, we associate the distinguished flag

$$\mathcal{V}(w) = \left(\mathbf{a}_{w(1)}, \mathbf{a}_{w(1)} \vee \mathbf{a}_{w(2)}, \ldots, \mathbf{a}_{w(1)} \vee \ldots \vee \mathbf{a}_{w(n+1)}\right),$$

where $\mathbf{a}_{i_1} \vee \mathbf{a}_{i_2} \vee \ldots \vee \mathbf{a}_{i_s}$ denotes the projective linear variety spanned by the points $\mathbf{a}_{i_1}, \mathbf{a}_{i_2}, \ldots, \mathbf{a}_{i_s}$. Notice that then B^w is the set of the flags in $\mathcal{F}lag(n+1)$ whose flag features have the same incidence relations with $\mathcal{V}$ as the flag features of $\mathcal{V}(w)$.

It is a classical result that each choice of a reference flag gives a stratification (in fact, cell decomposition) of the flag manifold:

Theorem 1 (Stratification of the flag manifold $\mathcal{F}lag(n+1)$). *(see [10] Ch. 13, Th. 4.3 or [9] Ch. 10): The disjoint union of all Bruhat cells B^w with $w \in \Sigma_{n+1}$ is a stratification for $\mathcal{F}\mathrm{lag}(n+1)$:*

$$\mathcal{F}\mathrm{lag}(n+1) = \cup_{w\in\Sigma_{n+1}} B^w \,. \tag{2}$$

The structure of each cell and the adjacency between them are also classically well established:

Proposition 1. *(see [10] Ch. 13, Prop. 4.7 or [9] Ch. 10, Prop. 7):*

1. *B^w is isomorphic to the affine space $\mathbb{R}^{\mathrm{length}(w)}$, where the* length *of a permutation w is defined as the number of inversions in w, that is,* $\mathrm{length}(w) = \#\{i < j : w(i) > w(j)\}$.

2. *If B^w and B^u are two cells of consecutive dimensions* $\mathrm{length}(w) = \mathrm{length}(u) + 1$, *then $\overline{B^w} \supset B^u$ if and only if there exists a transposition $t \in \Sigma_{n+1}$ such that $w = tu$.*

Example 1. *To illustrate the case $n = 3$, Fig. 1 shows the cells of dimensions 6 and 5 and their adjacencies. The rectangle represents the 6D cell $B^{(4,3,2,1)}$, while the ellipses are the 5D cells: $B^{(4,3,1,2)}$, $B^{(3,4,2,1)}$ and $B^{(4,2,3,1)}$. Each 5D cell is labelled also with $v-p^*$, $p-v^*$ and $l\cdot l^*$, respectively, which characterize the incidence relations between the flag features of the flags $v^* \subset l^* \subset p^* \subset \mathbb{P}^3$ in each cell and those of the reference flag $v \subset l \subset p \subset \mathbb{P}^3$. Note that v, l and p stand for vertex, line and plane, respectively, to ease recall. A hyphen between two elements denotes that one is included in the other, and a dot means that they meet at a single point.*

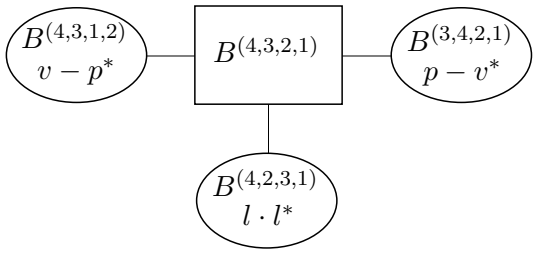

Figure 1: Adjacency between the higher dimensional cells of the flag manifold F*lag*(4): the rectangle represents the 6D cell, and the ellipses are the 5D cells.

To describe for which pairs u and w of permutations the stratum B^u is contained in the closure of B^w, the *Ehresmann-Bruhat order* is defined in the set Σ_{n+1}: $u \leq w$ if, and only if, there is sequence of transpositions $(j_1, k_1), \ldots, (j_r, k_r)$ with $j_i < k_i$ for all i connecting w and u (i.e. if we set $w_0 = w$ and $w_i = w \cdot (j_1, k_1) \cdot \cdots \cdot (j_i, k_i)$ then $w_r = u$) and satisfying $w_{i-1}(j_i) > w_{i-1}(k_i)$ at each step $1 \leq i \leq r$.

Remark 1. *(see [9] 10.5): A canonical way to construct such a sequence from w to u is as follows: for $1 \leq i \leq r$ take j_i as the smallest integer such that $w_i(j_i) > u(j_i)$, and k_i as the smallest integer greater than j_i such that $w_i(j_i) > w_i(k_i) \geq u(j_i)$. This procedure can be carried out for any w and u, and if the chain does not arrive at u, then u is not less than w in the Ehresmann-Bruhat order. For example, if $n = 3$, $w = (4, 2, 3, 1)$ and $u = (2, 1, 4, 3)$, then the canonical sequence is*

$$w = (\underline{4}, \underline{2}, 3, 1) \geq (2, \underline{4}, \underline{3}, 1) \geq (2, \underline{3}, 4, \underline{1}) \geq (2, 1, 4, 3) = u \ ,$$

where the pair switched at the next step is underlined. Besides, the first step shows, for example, that $w \not\geq (3, 4, 1, 2)$.

Proposition 2. *(see [9] 10.5): For u and v in Σ_{n+1}, the following are equivalent:*

1. *$u \leq v$,*
2. *$r_u(p, q) \geq r_v(p, q)$ for all p and q,*
3. *$B^u \subset \overline{B^v}$.*

Let us show that some stratifications of the flag manifold $\mathcal{F}lag(n+1)$ induce a stratification of the set of affine flags $\mathcal{F}_{\mathcal{A}}(\mathbb{P}^n)$. Fix from now on an affine reference flag, that is, $V_0 \subset \ldots \subset V_n = \mathbb{P}^n$ with $V_0 \notin H_\infty$. Consider the corresponding cell decomposition of $\mathcal{F}lag(n+1)$ as in (2). When restricted to the open subset of the affine flags $\mathcal{F}_{\mathcal{A}}(\mathbb{P}^n)$ the partition (2) clearly induces a partition:

$$\mathcal{F}_{\mathcal{A}}(\mathbb{P}^n) = \cup_{w \in \Sigma_{n+1}} (B^w \cap \mathcal{F}_{\mathcal{A}}(\mathbb{P}^n)). \tag{3}$$

Since the reference flag is an affine flag, none of the above intersections is empty. However it might happen that some cell B^w would split off into two connected components: indeed, $B^w \cap \mathcal{F}_{\mathcal{A}}(\mathbb{P}^n)$ is a unique connected component if and only if the permutation w starts with $w(1) = 1$. To see this,

choose an affine reference frame $\{V_0; \mathbf{e}_1, \ldots, \mathbf{e}_n\}$ attached to the reference flag, where $\mathbf{e}_1$ is a vector representing the improper point $\mathbf{e}_1^\infty = V_1 \cap H_\infty$, $\mathbf{e}_2$ is a vector representing another point $\mathbf{e}_2^\infty$ on the improper line $V_2 \cap H_\infty$, and so on. Let $(x_1, \ldots, x_n)$ denote the projective coordinates in its associated projective reference $\{V_0, \mathbf{e}_1^\infty, \ldots, \mathbf{e}_n^\infty; \mathbf{a}\}$.

First, let us give a construction of the isomorphism of Proposition 1. We say that a $(n+1)\times(n+1)$ matrix $\mathbf{M}$ *represents* a flag $\mathcal{V}^* = (V_0^*, \ldots, V_n^*) \in B^w$ if the first n rows of $\mathbf{M}$ span the flag features of $\mathcal{V}^*$, and the whole of its rows span $V_n^* = \mathbb{P}^n$. Observe that there is a unique $(n+1) \times (n+1)$ matrix $\mathbf{M}$ representing the flag $\mathcal{V}^*$ and satisfying the extra requirement that, for any $1 \leq p \leq n+1$, its p-th row has a 1 in the $w(p)$-th column, with all 0's at the right and below of this 1. This $\mathbf{M}$ will be called the *canonical matrix* representing the flag $\mathcal{V}^*$. For example, for $n = 3$ and $w = (3, 4, 2, 1)$ the cell B^w is isomorphic to the set of matrices of the form

$$\begin{pmatrix} * & * & 1 & 0 \\ * & * & 0 & 1 \\ * & 1 & 0 & 0 \\ 1 & 0 & 0 & 0 \end{pmatrix},$$

where the stars denote arbitrary real numbers; in this case B^w is the set of all flags whose vertex lies on the plane $V_2 : \{x_4 = 0\}$. The number of stars appearing in the canonical matrices parameterizing the flags of B^w (for an arbitrary w) turns out to be the length of w (see [9] 10.2).

If we switch to affine flags and we take up again the example of the permutation $w = (3, 4, 2, 1)$, the affine flags of B^w are the disjoint union of two strata: one of them is isomorphic to the set of matrices of the form

$$\begin{pmatrix} a & * & 1 & 0 \\ * & * & 0 & 1 \\ * & 1 & 0 & 0 \\ 1 & 0 & 0 & 0 \end{pmatrix}, \tag{4}$$

where the stars denote arbitrary real numbers and a denotes a positive real number; the other stratum is isomorphic to the set of matrices of the same form (4) where the stars denote arbitrary real numbers and a denotes a negative real number. The matrices of the form (4) where a is zero correspond to flags which are not affine.

For a permutation w with $w(1) > 1$, let B_+^w denote the connected component of $B^w \cap \mathcal{F}_\mathcal{A}(\mathbb{P}^n)$ formed from the flags $\{(V_0^*, \ldots, V_n^*) \in B^w : V_0^* =$

$(x_1, \ldots, x_{n+1})$ with $x_1 x_{w(1)} > 0\}$ and let B^w_- equal $\{(V_0^*, \ldots, V_n^*) \in B^w : V_0^* = (x_1, \ldots, x_{n+1})$ with $x_1 x_{w(1)} < 0\}$. Observe that the quotient $\frac{x_1}{x_{w(1)}}$ is the $(1,1)$ entry of the canonical matrix of any flag belonging to B^w. If $w(1) = 1$, set $B^w_+ = B^w_- = B^w$.

The interesting point of partition (3) is that it provides a stratification of $\mathcal{F}_{\mathcal{A}}(\mathbb{P}^n)$ and that the adjacency between the strata may also be determined by considering a refinement of the Ehresmann-Bruhat order:

Theorem 2. *1. The partition*

$$\mathcal{F}_{\mathcal{A}}(\mathbb{P}^n) = \bigcup_{\substack{w \in \Sigma_{n+1} \\ w(1) \neq 1}} (B^w_+ \cup B^w_-) \cup \bigcup_{\substack{w \in \Sigma_{n+1} \\ w(1) = 1}} B^w \tag{5}$$

is a stratification for the affine flags.

2. Let u and w be two permutations of Σ_{n+1}.

(a) If $u \leq w$, then $B^u_+ \subseteq \overline{B^w_+}$ and $B^u_- \subseteq \overline{B^w_-}$.

(b) If $u \leq w$ and $u(1) < w(1)$, then $B^u_+ \subseteq \overline{B^w_-}$ and $B^u_- \subseteq \overline{B^w_+}$.

(c) If $B^u_\varepsilon \cap \overline{B^w_{\varepsilon'}} \neq \emptyset$, then $u \leq w$. If moreover $\varepsilon \neq \varepsilon'$, then $u(1) < w(1)$ also holds. That is, there are no other adjacency between strata than those determined in (a) and (b).

Proof. We will prove Assertion 2, since it directly implies Assertion 1. Let $u, w \in \Sigma_{n+1}$ be two permutations such that $u \leq w$. Reasoning by induction on the finite number of transpositions connecting u and w, we need only to consider the case where $u = w \cdot (j,k)$, with $j < k$ and $w(j) = u(k) > w(k) = u(j)$. Take first any flag $E \in B^u_+$ and suppose $\mathbf{M}$ is its canonical matrix; we will show that $E \in \overline{B}^w_+$ and, if $u(1) < w(1)$ (i.e., $j = 1$), then also $E \in \overline{B}^w_-$.

In the sequel, if $\mathbf{A}$ is a matrix, its i-th row will be denoted by $\mathbf{a}^i$, its j-th column by $\mathbf{a}_j$, and its element in the i-th row and the j-th column by a^i_j. Since $E \in B^u$, there is an unipotent lower triangular matrix, denoted by $\mathbf{L}$, such that $\mathbf{M} = \mathbf{M}_{\mathcal{V}(u)}\mathbf{L}$, where $\mathbf{M}_{\mathcal{V}(u)}$ is the canonical matrix representing the flag $\mathcal{V}(u)$. Moreover, as $m^1_1 = l^{u(1)}_1$ and $E \in B^u_+$, it follows that $l^{u(1)}_1 > 0$.

Consider now, for any $t \in \mathbb{R}$, $t \neq 0$, the flag $G(t)$ represented by the

matrix $\mathbf{B}$ whose rows are as follows:

$$\begin{aligned} \mathbf{b}^i(t) &= \mathbf{e}_{w(i)} &&= \mathbf{e}_{u(i)} \ , && \text{for } i \neq j,k, \\ \mathbf{b}^j(t) &= t(\tfrac{1}{t}\mathbf{e}_{w(k)} + \mathbf{e}_{w(j)}) &&= \mathbf{e}_{u(j)} + t\mathbf{e}_{u(k)} \ , && (6) \\ \mathbf{b}^k(t) &= -\tfrac{1}{t}(\mathbf{e}_{w(k)} - \mathbf{b}^j(t)) &&= \mathbf{e}_{u(k)} \ , \end{aligned}$$

where $\mathbf{e}_i \in \mathbb{R}^{n+1}$ is the vector all whose components are zero but for the i-th one, which equals one. On the one hand, from the first expression, it follows that $G(t) \in B^w$ for any $t \in \mathbb{R}$, $t \neq 0$. On the other hand, the rightmost expression shows that the limit of $G(t)$ is the flag $\mathcal{V}(u)$ as $t \to 0$. Therefore the flag $F(t)$ represented by the matrix $\mathbf{A}(t) = \mathbf{B}(t)\mathbf{L}$ also belongs to B^w for all nonzero t, and the limit of $F(t)$ is the flag E as $t \to 0$. The last step that remains to be proved is whether $F(t) \in B^w_+$, i.e., $a^1_1(t)a^1_{w(1)}(t) > 0$. There are two possibilities:

- $w(1) = u(1)$. In this case, $j, k > 1$. Then we have, on one side,

  $$a^1_1(t) = \mathbf{b}^1(t)\mathbf{l}_1 = \mathbf{e}_{u(1)}\mathbf{l}_1 = l_1^{u(1)} \ ,$$

  which is positive by hypothesis. On the other side,

  $$a^1_{w(1)}(t) = \mathbf{b}^1(t)\mathbf{l}_{w(1)} = \mathbf{e}_{u(1)}\mathbf{l}_{u(1)} = l^{u(1)}_{u(1)} = 1 \ ,$$

  since $\mathbf{L}$ is unipotent. Therefore

  $$a^1_1(t)a^1_{w(1)}(t) = l_1^{u(1)} > 0 \ .$$

  This shows $F(t) \in B^w_+$ for any nonzero $t \in \mathbb{R}$, and thus $E \in \overline{B}^w_+$.

- $w(1) > u(1)$. This means $j = 1$, and then

  $$a^1_1(t) = \mathbf{b}^1(t)\mathbf{l}_1 = (\mathbf{e}_{u(1)} + t\mathbf{e}_{w(1)})\mathbf{l}_1 = l_1^{u(1)} + tl_1^{w(1)} \ ,$$

  $$a^1_{w(1)}(t) = \mathbf{b}^1(t)\mathbf{l}_{w(1)} = (\mathbf{e}_{u(1)} + t\mathbf{e}_{w(1)})\mathbf{l}_{w(1)} = l^{u(1)}_{w(1)} + tl^{w(1)}_{w(1)} = t \ ,$$

  since $\mathbf{L}$ is lower triangular and unipotent. Hence

  $$a^1_1(t)a^1_{w(1)}(t) = tl_1^{u(1)} + t^2 l^{w(1)}_{u(1)} \ .$$

  Recall that $l_1^{u(1)}$ is positive by hypothesis. Thus, if $t \to 0^+$ the value of $a^1_1(t)a^1_{w(1)}(t)$ is positive, and then $F(t) \in B^w_+$; but if $t \to 0^-$ the value is negative and $F(t) \in B^w_-$. Therefore, in this case both inclusions $E \in \overline{B}^w_+$ and $E \in \overline{B}^w_-$ hold.

If we start the reasoning for any $E \in B^w_-$, the proof is analogous, since now we have $l_1^{u(1)} < 0$, but for the case $u(1) = 1$, for which $l_1^{u(1)} = 1 > 0$. This exceptional case is handled similarly, taking into account that $B^u_+ = B^u_-$, when $u(1) = 1$.

Claims (a) and (b) being proved, it remains to show that there are no other adjacency relations between the strata. If $u \not\leq w$, in virtue of Proposition 2, we know that $B^u \not\subseteq \overline{B}^w$, and this implies that $B^u_a \not\subseteq \overline{B}^w_b$ for any $a, b \in \{+, -\}$. If $u \leq w$ and $u(1) = w(1)$, assume that there is a flag $E \in B^u_+ \cap \overline{B}^w_-$. Since $E \in \overline{B}^w_-$, there is a sequence $\{F_m\}_m \subseteq B^w_-$ of flags whose limit is E as $m \to \infty$. Looking at the vertices of these flags, we have a sequence of projective coordinates of points $\mathbf{v}_m = (v^i_m)$, for which $v^1_m v^{w(1)}_m < 0$, whose limit as $m \to \infty$ is $\mathbf{v} = (v^i)$, which satisfies $v^1 v^{u(1)} = v^1 v^{w(1)} > 0$, which is impossible. Thus $B^u_+ \cap \overline{B}^w_- = \emptyset$. Analogously $B^u_- \cap \overline{B}^w_+ = \emptyset$, and this completes the proof. □

Example 2. *To illustrate the case $n = 3$, Fig. 2 shows the strata of dimensions 6 and 5 of $\mathcal{F}_{\mathcal{A}}(\mathbb{P}^3)$ and their adjacency. The rectangles represents the two 6D strata $B^{(4,3,2,1)}_+$ and $B^{(4,3,2,1)}_-$, while the ellipses are the six 5D strata: $B^{(4,3,1,2)}_\varepsilon$, $B^{(3,4,2,1)}_\epsilon$ and $B^{(4,2,3,1)}_\varepsilon$, with $\varepsilon \in \{+, -\}$. For the sake of clarity, each 5D stratum is labelled also with $(v - p^*)^\varepsilon$, $(p - v^*)^\varepsilon$ and $(l \cdot l^*)^\varepsilon$, respectively, to make explicit the incidence relations between the flag features of the flags $v^* \subset l^* \subset p^* \subset \mathbb{P}^3$ in each stratum and those of the reference flag $v \subset l \subset p \subset \mathbb{P}^3$.*

3 Stratification of $\mathbb{R}^3 \times \mathbf{SO}(3)$ and adjacencies between the higher dimensional strata

In the sequel we restrict to the case $n = 3$. Consider an Euclidean reference frame attached to a given flag $\mathcal{V}^*$. Observe that the group of Euclidean transformations leaving this flag invariant is $\mathcal{H}_{\mathcal{V}^*} = \{\mathbf{I}, \mathbf{R}_x, \mathbf{R}_y, \mathbf{R}_z\}$, where $\mathbf{I}$ is the identity transformation, and $\mathbf{R}_k$ stands for a rotation of π radians about the k-axis (in the above mentioned reference frame attached to $\mathcal{V}^*$).

Fixed an affine reference flag $\mathcal{V}$, any $\mathbf{q} \in \mathbb{R}^3 \times \mathrm{SO}(3)$ defines a unique flag $\mathbf{q}(\mathcal{V})$. On the other hand, for any flag $\mathcal{V}^*$, there is some $\mathbf{q} \in \mathbb{R}^3 \times \mathrm{SO}(3)$ such that $\mathbf{q}(\mathcal{V}) = \mathcal{V}^*$. In fact, the set of 4 configurations yielding this same flag $\mathcal{V}^*$ is $\{\mathbf{Tq} \mid \mathbf{T} \in \mathcal{H}_{\mathcal{V}^*}\}$. This gives a four-fold covering morphism $\pi : \mathbb{R}^3 \times$

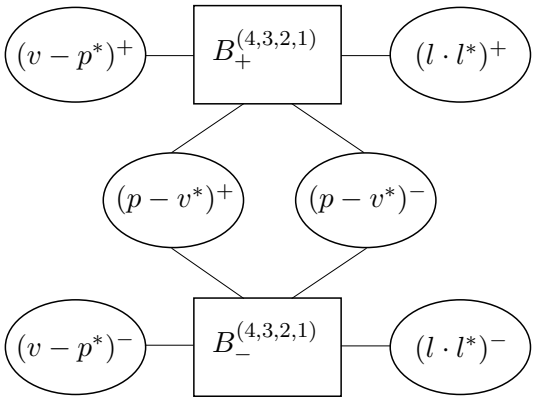

Figure 2: Adjacency between the higher dimensional strata of the set of affine flags $\mathcal{F}_{\mathcal{A}}(\mathbb{P}^3)$: the rectangles represent the 6D strata, and the ellipses are the 5D strata.

$\mathrm{SO}(3) \to \mathcal{F}_{\mathcal{A}}(\mathbb{P}^3)$[1] sending $\mathbf{q}$ to $\mathbf{q}(\mathcal{V})$ [17]. Via this 4-fold covering morphism π, the stratification of $\mathcal{F}_{\mathcal{A}}(\mathbb{P}^3)$ induces a stratification of $\mathbb{R}^3 \times \mathrm{SO}(3)$. For instance, via π, the two 6-dimensional disjoint strata of $\mathcal{F}_{\mathcal{A}}(\mathbb{P}^3)$ correspond in $\mathbb{R}^3 \times \mathrm{SO}(3)$ to 8 6D strata, that is, 8 connected components. Analogously, the 6 5D strata of $\mathcal{F}_{\mathcal{A}}(\mathbb{P}^3)$, correspond to 24 5D strata in $\mathbb{R}^3 \times \mathrm{SO}(3)$. We say that a 5D stratum of $\mathbb{R}^3 \times \mathrm{SO}(3)$ is *of type* $v^* - p$, $v - p^*$ or $l \cdot l^*$ if it is one of the connected components of the inverse image of a stratum $(v^* - p)^\varepsilon$, $(v - p^*)^\varepsilon$ or $(l \cdot l^*)^\varepsilon$, respectively, for some $\varepsilon \in \{+, -\}$ (see notation of Example 2). We shall focus on these strata of dimensions 5 and 6 and in determining their adjacency. To this aim we need to recall some concepts and results on paths and path lifting.

Definition 2. *A path in a manifold S is a continuous map γ from the unit real interval $[0, 1]$ to S; $\gamma(0)$ and $\gamma(1)$ are called the origin and end, respectively, of γ; γ is also called transition between $\gamma(0)$ and $\gamma(1)$. The path is closed if $\gamma(0) = \gamma(1)$. The inverse path of γ is defined as $\gamma^{-1}(t) = \gamma(1 - t)$.*

Given a covering morphism $\pi : \widetilde{S} \to S$, a lift of the path $\gamma : [0, 1] \to S$ is a path on $\widetilde{S}$, $\widetilde{\gamma} : [0, 1] \to \widetilde{S}$, such that $\pi \circ \widetilde{\gamma} = \gamma$.

Theorem 3 (Unicity of the lifting; see [13] 17.6). *Let $\pi : \widetilde{S} \to S$ be a covering morphism. Given a path $\gamma : [0, 1] \to S$ and a point $x \in \widetilde{S}$ such that*

[1] This morphism corresponds to the restriction of what is known as the four-fold covering morphism between the partially oriented flag manifold $G(1, 1 \mid 1, 1)$ in $\mathbb{P}^3$ and $\mathcal{F}lag(4)$ [17].

$\pi(x) = \gamma(0)$, *there is a unique lift* $\widetilde{\gamma}$ *of the path* γ *such that* $\widetilde{\gamma}(0) = x$.

To characterize each of the 8 6D strata of $\mathbb{R}^3 \times \mathrm{SO}(3)$ we use the triple of signs corresponding to the orientation of the three tetrahedra defined as follows. Suppose that the flag features of the affine reference flag $\mathcal{V}$ are spanned by three affine points $\mathbf{a}_1, \mathbf{a}_2, \mathbf{a}_3$, that is, $\mathcal{V} = (\mathbf{a}_1, \mathbf{a}_1 \vee \mathbf{a}_2, \mathbf{a}_1 \vee \mathbf{a}_2 \vee \mathbf{a}_3, \mathbb{P}^3)$. Given $\mathbf{q} \in \mathbb{R}^3 \times \mathrm{SO}(3)$, consider the points $\mathbf{b}_i = \mathbf{q}(\mathbf{a}_i)$ for $1 \leq i \leq 3$. Observe that $\mathbf{q}$ lies on a 5D stratum if, and only if, $\mathbf{b}_1$ lies on the plane $\mathbf{a}_1 \vee \mathbf{a}_2 \vee \mathbf{a}_3$, the lines $\mathbf{a}_1 \vee \mathbf{a}_2$ and $\mathbf{b}_1 \vee \mathbf{b}_2$ intersect, or $\mathbf{a}_1$ lies on the plane $\mathbf{b}_1 \vee \mathbf{b}_2 \vee \mathbf{b}_3$. Equivalently, $\mathbf{q}$ lies on a 6D stratum if, and only if, the points in the sets

$$\{\mathbf{a}_1, \mathbf{a}_2, \mathbf{a}_3, \mathbf{b}_1\},\ \{\mathbf{a}_2, \mathbf{a}_3, \mathbf{b}_1, \mathbf{b}_3\},\ \{\mathbf{a}_3, \mathbf{b}_1, \mathbf{b}_2, \mathbf{b}_3\} \tag{7}$$

form three non-degenerate tetrahedra. The orientation of a non-degenerate tetrahedron is given by the sign of the determinant of the matrix whose rows are the coordinates of the vertices of the tetrahedron. Hence, by assigning to any $\mathbf{q} \in \mathbb{R}^3 \times \mathrm{SO}(3)$ the triple of signs corresponding to the orientation of its three associated tetrahedra, we obtain a partition of the 6D strata into 8 disjoint open sets which, by connectivity arguments, must correspond to the 8 6D strata. Notice that the four 6D strata $(\varepsilon, +, +)$, $(\varepsilon, +, -)$, $(\varepsilon, -, +)$ and $(\varepsilon, -, -)$ map by the covering π to $B_\varepsilon^{(4,3,2,1)}$ for $\varepsilon \in \{+, -\}$.

Theorem 4. *Each pair of 6D strata of* $\mathbb{R}^3 \times SO(3)$ *differing in only one sign are separated by two different 5D strata which are both of type* $p - v^*$, $l \cdot l^*$ *or* $v - p^*$, *if the differing sign occupies the first, second or third position, respectively.*

Proof. Directly due to the 4-fold covering π, there are two different 5D strata of type $p - v^*$ separating each pair of 6D strata $(+, \varepsilon_1, \varepsilon_2)$ and $(-, \varepsilon_1, \varepsilon_2)$ for any $\varepsilon_1, \varepsilon_2 \in \{+, -\}$. Fix a flag $\mathcal{V}^* = \mathbf{q}(\mathcal{V}) \in B_\varepsilon^{(4,3,2,1)}$, with $\varepsilon \in \{+, -\}$. We will consider in $\mathcal{F}_{\mathcal{A}}(\mathbb{P}^n)$ four different paths with origin $\mathcal{V}^*$ that will lie entirely in $B_\varepsilon^{(4,3,2,1)}$ except at a point, at which a 5D stratum will be crossed. Namely, ρ_x and ρ_z are the rotations from 0 to π radians about the x-axis and z-axis, respectively, of an Euclidean reference frame attached to the flag $\mathcal{V}^*$; ρ_x^{-1} and ρ_z^{-1} are the respective inverse paths, i.e., rotations from 0 to $-\pi$ radians. Observe that the path $\rho_x(t) = (v^*, l^*, p^*(t))$ crosses the 5D stratum $(v - p^*)^\varepsilon$ at the point $\rho_x(t_0) = (v^*, l^*, p^*(t_0))$ at which the platform plane $p^*(t_0)$ touches the vertex v of the base plane, and that $\rho_z(t) = (v^*, l^*(t), p^*)$

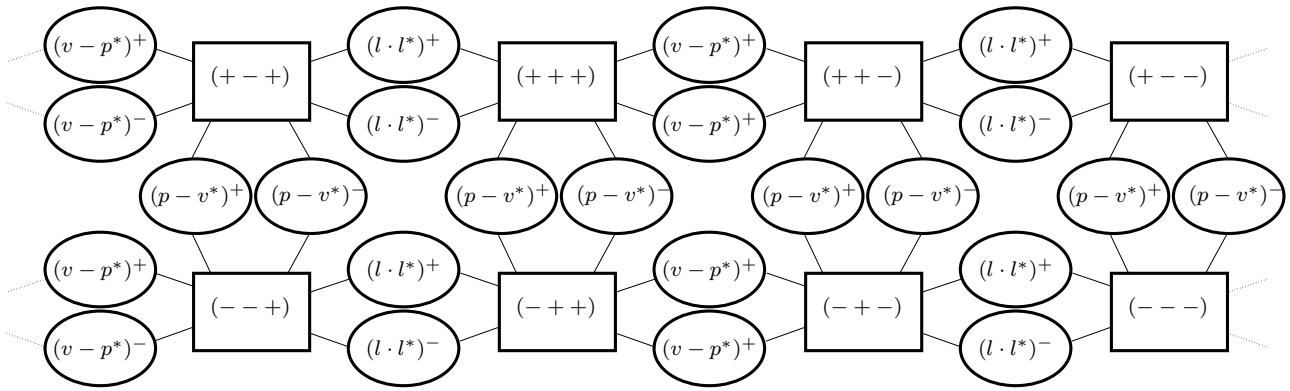

Figure 3: The graph shows the adjacency between the higher dimensional strata of the stratification of the Euclidean motion group. The rectangles represent the 6D strata, and the ellipses the 5D strata.

crosses the 5D stratum $(l \cdot l^*)^\varepsilon$ at the point $\rho_z(t_1) = (v^*, l^*(t_1), p^*)$ at which the platform line $l(t_1)$ goes through the point $p^* \cap l$.

Let $\{\mathbf{q}, \mathbf{R}_x\mathbf{q}, \mathbf{R}_y\mathbf{q}, \mathbf{R}_z\mathbf{q}\}$ be the 4 points in the fiber of $\mathcal{V}^* = \mathbf{q}(\mathcal{V})$. Consider the lifts of the paths ρ_x, ρ_x^{-1}, ρ_z and ρ_z^{-1} with origin $\mathbf{q}$ (cf. Theorem 3): $\widetilde{\rho_x}$, $\widetilde{\rho_x^{-1}}$, $\widetilde{\rho_z}$ and $\widetilde{\rho_z^{-1}}$. Notice that the transitions $\widetilde{\rho_x}$ and $\widetilde{\rho_x^{-1}}$ do not intersect except at the ends; the different configurations $\mathbf{q}_{t_0}$ and $\mathbf{q}'_{t_0}$ at which $\widetilde{\rho_x}$ and $\widetilde{\rho_x^{-1}}$, respectively, cross a 5D stratum share the same flag $\rho_x(t_0)$, that is, $\pi(\mathbf{q}_{t_0}) = \pi(\mathbf{q}'_{t_0}) = \rho_x(t_0)$; at $\mathbf{q}_{t_0}$ and $\mathbf{q}'_{t_0}$ the volume of the last tetrahedra appearing in (7) becomes zero. Hence each transition crosses a different 5D stratum in $\mathbb{R}^3 \times \mathrm{SO}(3)$ of type $v - p^*$ and both transitions join two 6D strata whose differing sign occupies the third position. An analogous reasoning applies for transitions $\widetilde{\rho_z}$ and $\widetilde{\rho_z^{-1}}$: each of them crosses a different 5D stratum in $\mathbb{R}^3 \times \mathrm{SO}(3)$ of type $l \cdot l^*$ and both transitions join two 6D strata whose differing sign occupies the second position. Finally a similar reasoning can be carried out with the lifts of the paths ρ_x and ρ_x^{-1} with origin $\mathbf{R}_z\mathbf{q}$, and with the lifts of the paths ρ_z and ρ_z^{-1} with origin $\mathbf{R}_x\mathbf{q}$ proving, thus completely, the statement of the Theorem and the adjacency displayed in Fig. 3. □

4 Applications to the kinematics of robots

Let us show that the stratification of the Euclidean motion group just inferred characterizes the singular locus of a wide class of spatial parallel manipulators, hence its significance for the design and control of parallel robots.

A parallel manipulator whose singularities can be described in terms of incidences between two flags adequately placed on its platform and base, respectively, is called a *flagged manipulator*. As an example, Figure 4 shows a parallel manipulator, known as 3/2 Hunt-Primrose manipulator [11], in a singular configuration characterized by the point v of the base flag lying on the line l^* of the platform flag.

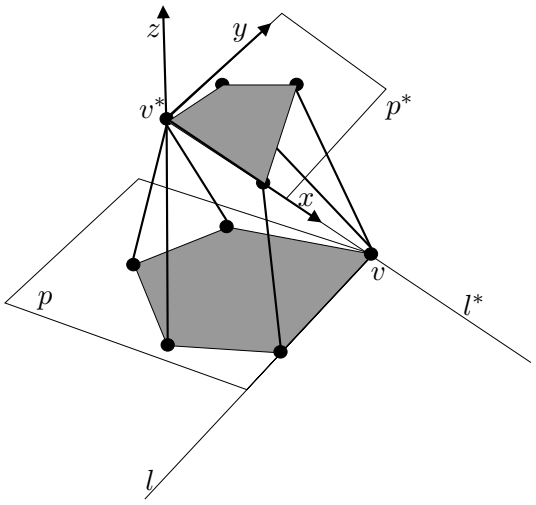

Figure 4: A singular configuration of a 3/2 Hunt-Primrose manipulator, in which two of the tetrahedra defining its forward kinematics are degenerate.

There are many different possible architectures for a spatial parallel manipulator, depending on the placement of the legs, from the most general ones, in which every leg endpoint is different, to others more specialized that have up to three legs sharing one endpoint. Clearly, the way the legs are placed has decisive influence when computing the position of the platform (with respect to the base) from the six lengths, and thus, when computing the singular locus. In [2], manipulator transformations that leave singularities invariant have been studied, which permit carrying out the singularity analysis on a single representative of each manipulator class and the obtained

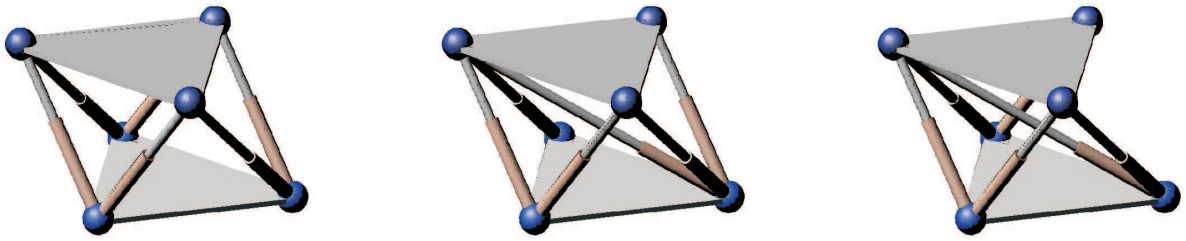

(a) **(b)** **(c)**

Figure 5: The three possible architectures for the 3-3 parallel manipulators: (a) octahedral, (b) flagged and (c) partially-flagged.

result is guaranteed to be valid for all transformed manipulators. For the sake of simplicity, the representative of the flagged parallel manipulators is chosen to have a 3-3 architecture. A 3-3 manipulator is a 6-legged parallel manipulator whose leg endpoints merge into three points (in practice, into three multiple spherical joints).

There are only three possible architectures for this kind of manipulators (refer to Fig. 5), namely the well-known octahedral manipulator, whose forward kinematics is not solvable in closed-form [8], the basic flagged manipulator studied in this paper, and the so far barely known partially-flagged manipulator, which will be the object of future work as mentioned in the next section.

By applying the singularity-preserving transformations mentioned above to the leg endpoint locations of the 3-3 flagged manipulator (Fig. 5(b)), the large family of 6-legged flagged manipulators has been expanded [4]. It consists of 39 architectures ranging from the 3-3 basic one up to a 6-6 parallel manipulator having five points aligned in both the platform and the base. In between, one finds some popular robot designs such as the 3/2 Hunt-Primrose manipulator [11], the $(3\text{-}1\text{-}1\text{-}1)^2$ manipulator [5], and several of the architectures studied by Zhang and Song [21]. All these designs had separately attracted attention in practice because their forward kinematics has a nice closed-form solution, which can now be interpreted in terms of incidences between two flags (see below).

Moreover, by replacing 2-leg groups by kinematically equivalent serial chains among the 144 identified by Ben-Horin and Shoham [3], the much

larger family of 3-legged flagged manipulators has also been derived (see details in [2]).

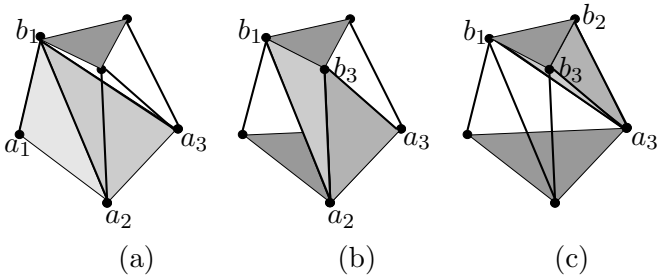

Figure 6: The tetrahedra involved in the computation of the forward kinematics of the parallel manipulator in Fig. 5(b).

Now, let us concentrate our attention on the forward kinematics of the basic flagged manipulator. Given the lengths of the legs $\overline{\mathbf{a}_1\mathbf{b}_1}$, $\overline{\mathbf{a}_2\mathbf{b}_1}$, and $\overline{\mathbf{a}_3\mathbf{b}_1}$, there are two possible mirror locations for $\mathbf{b}_1$ with respect to the plane defined by $\mathbf{a}_1$, $\mathbf{a}_2$, and $\mathbf{a}_3$ [Fig. 6(a)]. Once one of these two solutions for $\mathbf{b}_1$ is chosen, $\mathbf{a}_2$, $\mathbf{a}_3$, $\mathbf{b}_1$ and $\mathbf{b}_3$ define another tetrahedron with known edge lengths [Fig. 6(b)]. Again, there are two possible mirror locations for $\mathbf{b}_3$, in this case with respect to the plane defined by $\mathbf{a}_2$, $\mathbf{a}_3$, and $\mathbf{b}_1$. Finally, after choosing one of the two solutions, $\mathbf{a}_3$, $\mathbf{b}_1$, $\mathbf{b}_2$, and $\mathbf{b}_3$ define another tetrahedron with known edge lengths [Fig. 6(c)]. In this case there are also two mirror locations for $\mathbf{b}_2$ with respect to the plane defined by $\mathbf{b}_1$, $\mathbf{b}_3$ and $\mathbf{a}_3$. We conclude that if, and only if, the points in the sets $\{\mathbf{a}_1, \mathbf{a}_2, \mathbf{a}_3, \mathbf{b}_1\}$, $\{\mathbf{a}_2, \mathbf{a}_3, \mathbf{b}_1, \mathbf{b}_3\}$, and $\{\mathbf{a}_3, \mathbf{b}_1, \mathbf{b}_2, \mathbf{b}_3\}$ form non-degenerate tetrahedra, there are eight possible configurations for the moving platform compatible with a given set of leg lengths. Otherwise, the 6-tuple of leg lengths constitutes a bifurcation point of the map Φ (see Eq. (1)), that is, a value of leg lengths for which the number of ways of assembling the platform to the base changes, either increasing or decreasing.

By taking inverse images, the singularity locus of the manipulator is obtained. It can also be derived by computing the zero locus of the determinant of the analytic Jacobian of Φ [8], which is expressed as the product of the three determinants:

$$\det(\mathbf{a}_1, \mathbf{a}_2, \mathbf{a}_3, \mathbf{b}_1) \cdot \det(\mathbf{a}_2, \mathbf{a}_3, \mathbf{b}_1, \mathbf{b}_3) \cdot \det(\mathbf{a}_3, \mathbf{b}_1, \mathbf{b}_2, \mathbf{b}_3) = 0\,.$$

Thus, the manipulator is at a singularity if, and only if, $\mathbf{b}_1$ is on the base plane, the lines defined by $\mathbf{a}_2\mathbf{a}_3$ and $\mathbf{b}_1\mathbf{b}_3$ intersect, or $\mathbf{a}_3$ is on the platform

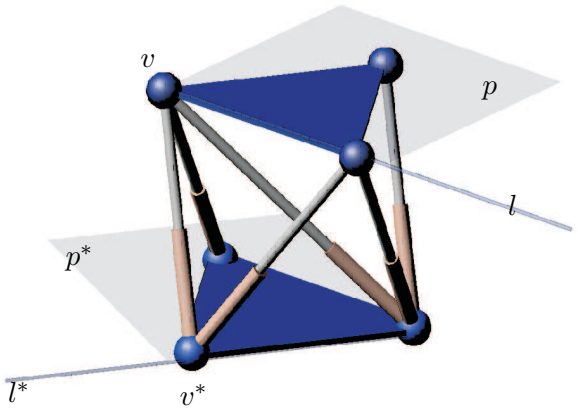

Figure 7: The basic flagged manipulator and its attached flags.

plane. Therefore, if two flags are placed on the manipulator base and platform as shown in Fig. 7, then the manipulator singularity locus coincide with flag configurations in which either the vertex of one flag lies on the plane of the other flag or the two flag lines intersect.

In sum, flagged parallel manipulators have singularity loci with a well-structured topology that has been studied in this paper. Of special interest in practice is the fact that each cell in the derived stratification can be characterized using a single local chart whose coordinates directly correspond to uncoupled translations and/or rotations in the workspace of the manipulator.

5 Future work and other applications

We are currently exploring the possibility of carrying out a similar analysis for the families of manipulators derived from other 3-3 parallel architectures.

In particular, the study of the 3-3 parallel architecture named *partially-flagged manipulator* (Fig. 5(c)) has led us to consider configurations of more than two flags and to study their topology, falling in the same stream as the recent works of [15] and [18]. Concretely, our work in progress uses the action of the linear group on the triple product of two flags and a point studied by Magyar in [15] and analyzes its restriction to a suitable submanifold, which parameterizes the relative positions (under linear transformations) between a flag (attached to the manipulator platform) and a pair (v, l), v a point

and l a line such that $v \nsubseteq l$ (attached to the manipulator base). The line l together with the plane spanned by l and v is interpreted as a *partial flag* (which is a sequence of subspaces, non necessarily of each dimension as is the case for a flag) and hence the name of partially-flagged manipulator.

We are now trying to follow steps of reasoning analogous to these developed in this paper in order to obtain an alternative stratification of the Euclidean motion group $\mathbb{R}^3 \times SO_3(\mathbb{R})$ coherent with the singularity set of the partially-flagged manipulator and its whole family derived from it. It is worth noticing that this new stratification of $\mathbb{R}^3 \times SO_3(\mathbb{R})$ is formed from completely different regions (for instance, no zero dimensional stratum appears), which are not even cells at the level of the flag manifold. However, this new stratification and the one obtained in the present paper have the same adjacency diagram of the 5 and 6 dimensional strata (see our Fig. 3), and we suspect that this higher dimensional adjacency diagram will be shared by the wide class of all trilaterable manipulators (i.e., manipulators whose forward kinematics can be solved by three consecutive trilateration operations).

Finally, let us mention that we envisage other applications of the developed stratifications outside of the robot kinematics field. They are related to collision detection and proximity queries between polyhedra in the domain of Computational Geometry [14, 12]. There are three types of basic contacts between two polyhedra [19], namely face-vertex, edge-edge, and vertex-face contacts. Now, by adequately attaching flags to the two polyhedra, each contact type corresponds to the degeneration of one the three tetrahedra in (7). Therefore, the three hypersurfaces in $\mathbb{R}^3 \times SO_3(\mathbb{R})$ defining the singularity loci for flagged manipulators are the same as those defining basic contacts between polyhedra. Moreover, strata of lower dimensions in the stratification correspond to multiple contacts. As an example, the flag configuration depicted in Fig. 4 entails a double vertex-plane $(v - p^*)$ and line-line $(l - l^*)$ contact, which boils down to a vertex v of one polyhedron impinging on an edge l^* of the other polyhedron.

Note, however, that this application is considerably more involved than the robot kinematics one, where two flags sufficed. Here one would have to consider flags for all vertices in the two polyhedra, and deal with the intersection of the induced stratifications in order to obtain an operative decomposition of the contact space between the polyhedra.

References

[1] M. Alberich-Carramiñana, F. Thomas and C. Torras, "On redundant flagged manipulators," *Proc. IEEE Intl. Conf. on Robotics and Automation (ICRA)*, Orlando, Fl., pp. 783-789, 2006.

[2] M. Alberich-Carramiñana, F. Thomas and C. Torras, "Flagged Parallel Manipulators," *IEEE Transactions on Robotics*, Vol. 23(5), pp. 1013-1023, 2007.

[3] P. Ben-Horin and M. Shoham, "Singularity condition of six-degree-of-freedom three-legged parallel robots based on grassmann-cayley algebra," *IEEE Transactions on Robotics*, Vol. 22(4), pp. 577-590, 2006.

[4] J. Borràs, F. Thomas and C. Torras, "Architecture singularities in flagged parallel manipulators," *Proc. IEEE Intl. Conf. on Robotics and Automation (ICRA)*, Pasadena, Ca., pp. 3844-3850, 2008.

[5] H. Bruyninckx, "Closed-form forward position kinematics for a $(3\text{-}1\text{-}1\text{-}1)^2$ fully parallel manipulator," *IEEE Transactions on Robotics and Automation*, Vol. 14(2), pp. 326-328, 1998.

[6] B. Dasgupta and T.S. Mruthyunjaya, "The Stewart Platform: a Review," *Mechanism and Machine Theory*, Vol. 35, pp. 15-40, 2000.

[7] P. S. Donelan, "Singularities of Robot Manipulators," *Procs. "5 Weeks in Singularities"*, ed. D. Trotman, World Scientific, 2007.

[8] D. M. Downing, A. E. Samuel, and K. H. Hunt, "Identification of the special configurations of the octahedral manipulator using the pure condition," *Intl. Journal of Robotics Research*, Vol. 21(2), pp. 147-160, 2002.

[9] W. Fulton, *Young Tableaux*, London Mathematical Society Student Texts 35, Cambridge University Press, Cambridge, 1997.

[10] H. Hiller, *Geometry of Coxeter Grups*, Research Notes in Mathematics, Pitman Books, London, 1982.

[11] K. H. Hunt and E. J. F. Primrose, "Assembly configurations of some in-parallel actuated manipulators," *Mechanism and Machine Theory*, Vol. 28(1), pp. 31-42, 1993.

[12] P. Jiménez, F. Thomas and C. Torras, "3D collision detection: a survey". *Computers and Graphics*, Vol. 25(2), pp. 269-285, 2001.

[13] C. Kosniowski, *A first course in algebraic topology*, Cambridge University Press, Cambridge-New York, 1980.

[14] M.C. Lin and D. Manocha, "Collision and Proximity Queries," in *Handbook of Discrete and Computational Geometry*, 2nd edition, Chapter 35, CRC Press, 2004.

[15] P. Magyar, "Bruhat order of two flags and a line," *Journal of Algebraic Combinatorics*, Vol. 21, pp. 71-101, 2005.

[16] D. Monk, "The Geometry of Flag Manifolds," *Proc. of the London Mathematical Society*, Vol. 9, No. 9, 1959.

[17] P. Sankaran and P. Zvengrowski, "Stable parallelizability of partially oriented flag manifolds II," *Can. J. Math*, Vol. 49, No. 6, pp. 1323-1339, 1997.

[18] E. Smirnov, "Bruhat order for two subspaces and a flag," *arXiv:0704.3061*, 2007.

[19] F. Thomas and C. Torras, "A projectively invariant intersection test for polyhedra," *Visual Computer*, Vol. 18(7), pp. 405-414, 2002.

[20] C. Torras, F. Thomas and M. Alberich-Carramiñana, "Stratifying the singularity loci of a class of parallel manipulators," *IEEE Transactions on Robotics*, Vol. 22(1), pp. 23-32, 2006.

[21] Ch. Zhang and S-M. Song, "Forward kinematics of a class of parallel (Stewart) platforms with closed-form solutions," *Proc. IEEE Intl. Conf. on Robotics and Automation*, pp. 2676-2681, 1991.